Comparison of CMIP5 and CMIP6 high-resolution simulations for soil erosion response to climate and land use changes over China

X. R. Weng [1], J. X. Zhu [1,*], D. G. Wang [1,*], S. Wang [2], and J. X. Qiu [1]

[1] School of Geography and Planning, Sun Yat-Sen University, Guangzhou, China.

[2] Department of Land Surveying and Geo-Informatics, The Hong Kong Polytechnic University, Hong Kong, China.

Corresponding author: Jinxin Zhu (zhujx29@mail.sysu.edu.cn); Dagang Wang (wangdag@mail.sysu.edu.cn)

Key Points:

- A comparison of soil erosion impacts using Coupled Model Intercomparison Project version 5 (CMIP5) and Phase 6 (CMIP6) high-resolution models is performed over China.
- CMIP6 model outperforms downscaled model from CMIP5 for better circulation simulations in terms of validation and project a less severe soil erosion future.
- It is recommended to update soil erosion impact studies performed using CMIP5 with the CMIP6 high-resolution models.

Abstract

Soil erosion is impacted by climate and land use changes which need to be quantified to assess future risks and to design efficient soil conservation measures. The Coupled Model Intercomparison Project Phase 5 (CMIP5) simulations have provided the basis for most such assessments and yet are being gradually superseded by more recent simulations from Phase 6 (CMIP6). The High-Resolution Model Intercomparison Project (HighResMIP) experiment in CMIP6 adds value over the downscaled CMIP5 simulations by improving process representation in the global climate system. Our study investigates and compares high-resolution model simulations from CMIP6 against CMIP5. Model evaluation for the reference period (1986–2005) indicates that the CMIP6 model outperforms the regional climate models (RCM) from CMIP5 for better circulation simulations, but both overestimate soil erosion in China. The average projected soil erosion for 2031–2050 relative to the historical period increases by 27.85 from CMIP5 and 20.03 $t \cdot hm^{-2} \cdot a^{-1}$ from the CMIP6 model with remarkable geographical heterogeneity. Soil erosion is projected to decrease in the black soil region, purple soil region, and karst region from CMIP6 results, which is opposite to the increasing trend found in those regions from CMIP5. Land use and climatic changes contributed 51.68% and -5.92% respectively from CMIP5 simulations while 35.74% and -13.77% from CMIP6 to the increased soil erosion rate. The negative contribution of land use change is gradually intensified with the CMIP6 model representing finer-scale processes of converting land-use type into cropland, pasture, and urban land. Overall, we assess that the CMIP6 projections provide a less severe soil erosion situation while addressing the need to pursue soil conservation more.

Plain Language Summary

Global warming is intensifying the hydrological cycle significantly, which in turn impacts soil erosion by water worldwide. It is essential to quantify these impacts to assess future risk and vulnerability. High-resolution climate models coupled with erosion models are the optimal tools to achieve this. The models from Coupled Model Intercomparison Project version 5 (CMIP5) have been downscaled to assess the impacts of climate change on rainfall erosivity over the past decade. The more recent sixth phase (CMIP6) has started to directly generate high-resolution projections, which brings the necessity of comparison between CMIP5 and CMIP6 in terms of performance and projection differences. Results show that the CMIP6 model outperforms the downscaled model from CMIP5 in terms of validation and projects a less severe soil erosion future. The high-resolution CMIP6 model adds value over the downscaled CMIP5 model by improving process representation in the global climate system. Soil erosion is projected to decrease in the black soil region, purple soil region, and karst region from CMIP6 results while the increase from CMIP5.

1 Introduction

According to the Global Assessment of Land Degradation (GLADA), about 1.1 billion hectares of global land have been degraded by soil erosion (Bai et al., 2008). Erosion removes the fertile topsoil, where most organic matter and nutrients are available. Naipal et al., (2018) estimated that accelerated soil erosion due to human activities has led to a total potential soil organic carbon loss of 74 Pg during the period 1850–2005, of which 79%–85% occurred in agricultural land and grassland. Moreover, soil erosion has been reported to cause annual socio-economic losses of approximately 40 billion dollars globally (Oldeman et al., 1990; Crosson, 1995). Now, coupled with the rapid changes in land use and climate, these problems will worsen. A recent study found that both land use and climate change contributing to global soil erosion by water would increase by 30%–66% by 2070 (Borrelli et al., 2020). Hence, projecting this variability well in advance can more effectively guide the government to take measures to control soil degradation, protect the ecological environment, and provide a theoretical reference for realizing the sustainable utilization of land resources. A modeling approach, climate models with different climate scenarios combined with erosion models, is a common and useful way to project soil erosion under climate change (Zhi et al., 2011). However, the previous model simulation is based on the framework of CMIP5. With the introduction of new CMIP6 and SSP scenarios, the issue of revisiting soil erosion simulations and projections is raised.

Over the past few decades, progress in climate modeling has provided new insight regarding soil erosion. The potential effects of climate change on erosion have been studied using different integrated modeling frameworks consisting of hydrologic/erosion, climate, and land use models(Maeda et al., 2010b; Borrelli et al., 2020; Eekhout and Vente, 2022; Luetzenburg et al., 2020; Maeda et al., 2010a; Pal et al., 2021). In order to incorporate the impacts of future climate change, a multi-model, multi-scenario approach with various global climate models (GCMs) is often combined with the Revised Universal Soil Loss Equation (RUSLE). GCMs can simulate the effects of greenhouse gas (GHG) emissions on climatic systems and realistically predict future conditions (Hartmann, 2016). The essential climatic variables obtained from GCMs simulations are used as input data to RUSLE to assess the possible impacts of climate change on soil erosion. These GCMs are available publicly as part of the Coupled Model Intercomparison Project (CMIP). However, the resolution of GCMs is too coarse to feed the erosion models (Rivington et al., 2008). The resolution of the model plays an important role in the reliability of the final results. Meanwhile, extreme events are responsible for high soil erosion rates, the GCMs do not capture these extremes. The high-resolution regional climate models (RCMs) are superior to that GCMs to capture a more realistic local forcing such as complex topography and land surface heterogeneity (Nikiema et al., 2017; Vizy et al., 2013). Recently, the continuous efforts to develop model resolution and physics have shown advancement in rainfall and land use simulation in the CMIP6 models relative to the CMIP5 and CMIP3 models. The CMIP6 model forecasts additional scenarios using shared socioeconomic pathways (SSPs) (O'Neill et al., 2016; Schlund et al., 2020). These updated climate projections take socioeconomic developments, technological advancement, and other environmental factors (such as land use) into account (Moss et al., 2010), enabling the development of new scenarios to better evaluate the consequences of climate change policies. The CMIP6 is the ideal framework for conducting studies of a large multi-model ensemble with a higher resolution. The High-Resolution Model Intercomparison Project (HighResMIP) experiments within the CMIP6 models (Haarsma et al., 2016), for the first time, were conducted with resolutions of at least 50 km in the atmosphere and 0.25° in the ocean. These experiments provide an opportunity to understand the hydrological cycle and its variability based on global high-resolution multi-model ensemble

simulation. Compared with CMIP5, CMIP6 (coarse resolution and HighResMIP experiments) models show an improvement in bias reduction of extreme precipitation over Asia (Dong and Dong, 2021), particularly for HighResMIP in the simulation of precipitation distribution in China (Xin et al., 2021). Therefore, the investigation of the impact of land use and climate change on soil erosion based on these recently released model projections and the horizontal comparison with the results of CMIP5 high-resolution RCMs has not been performed. Hence, more studies showing the benefit obtained from the improvement of CMIP6 compared with the CMIP5 framework affecting the research on soil erosion are needed.

This study has two main objectives: (1) Through the selected CMIP6 high-resolution GCM and CMIP5 high-resolution RCM, combined with land use change data and RUSLE model, the impacts and differences of climate change and land use change on soil erosion in China under the two frameworks are comprehensively analyzed and compared. The future estimation of soil and water loss under RCPS and SSPs scenarios is studied. (2) The control variable method is used to quantitatively analyze the difference in the contribution rate of climate change and land use change to soil erosion under the two frameworks, and to analyze the underlying mechanism and reasons. This effort will assist local authorities to pinpoint current and future problematic soil erosion rates at the highest resolution possible, in support of measures to conserve soil resources. Assessment of the simulated relationship from the recent two generations of CMIP will also provide new insight for the scientific community in model development.

2 Data and Methods

2.1 Study area

China is located on the east side of the Eurasian continent and the west coast of the Pacific Ocean, geographically ranging from 73°33'E to 135°05'E and 3°51'N to 53°33'N. The huge undulation of topography, numerous mountains and hills, and complex and diverse strata, especially the Quaternary loose sediments and slightly cemented clastic rocks that are widely covered, provide conditions for soil erosion. Precipitation is the basic dynamic condition for the occurrence and development of hydraulic erosion. China has obvious monsoons and strong continental characteristics. Precipitation is concentrated, rain and heat are in the same season, and the water and heat conditions from the southeast coast to the northwest inland are different in space. The precipitation in most parts of the country is concentrated from June to August, and the precipitation decreases from southeast to northwest. The surface composition, soil, and its parent material are the material sources of soil erosion. The soil types in China are diverse and show a zonal distribution pattern, which is closely related to the occurrence and distribution of soil erosion. Vegetation is an important factor affecting soil erosion. The zonal distribution of vegetation in China is obvious. Due to the gradual reduction of precipitation from coastal to inland, the landscape features from forest to grassland and then to the desert are formed, reflecting the law of regional differentiation from coastal to inland. In addition, China's social and economic development is unbalanced, the economic development intensity in the eastern region is high, a large amount of agricultural land is converted into construction land, and artificial soil erosion is relatively serious. The problems of grassland overload and land desertification and degradation are prominent in the western region. Excessive land reclamation still exists in Southwest China, and soil erosion of sloping farmland is very serious. Frequent rainstorms, dense population distribution, and frequent production activities lead to obvious differences in soil erosion types and distributions in China. According to the Soil Erosion Classification Standard of China established by the Ministry of Water Resources, the study area is divided into the following eight water and soil conservation areas, as

shown in Fig.1

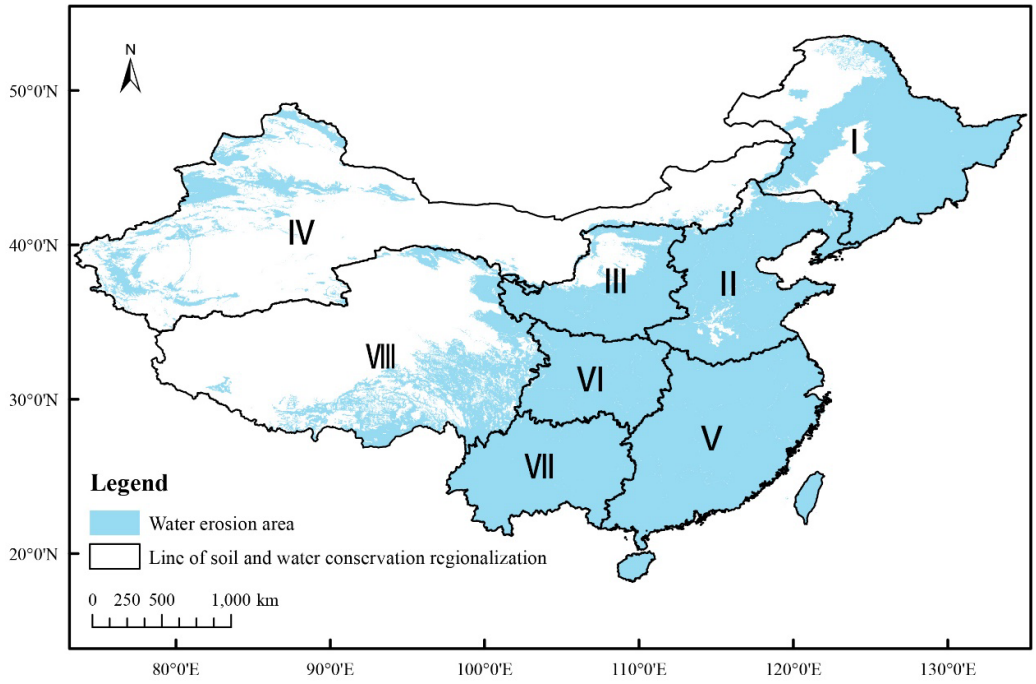

Fig.1 The eight soil and water conservation areas in mainland China: Northeast China black soil region (I), North China mountainous region (II), Northwest China Loess Plateau region (III), North China sandstorm region (IV), South China red soil region (V), Southwest China purple soil region (VI), Southwest China karst region (VII) and Qinghai-Tibet Plateau region (VIII)

2.2 Datasets

The simulated daily precipitation data are retrieved from the MPI-M-MPI-ESM-LR of CORDEX (https://esg-dn1.nsc.liu.se/search/cordex/) and MPI-ESM1.2-XR of CMIP6 (https://esgf-node.llnl.gov/search/cmip6/). Both models have been developed by the Max Planck Institute for Meteorology (MPI-M), Germany. They shared the same parent dynamical core structure, parameterizations, simulation variant, and spatial resolution (50km). MPI-ESM1.2-XR is obtained from the control runs of a model taking part in the High-Resolution Model Intercomparison Project (HighResMIP) within the CMIP6 protocol. HighResMIP aims to study improvement in climate model simulation performance with increased horizontal resolution and to reduce simulation uncertainty based on multi-model ensemble simulation (Haarsma et al., 2016). High-resolution models are more capable of representing diurnally forced circulations and modulated rainfall due to orography (Boyle and Klein, 2010). We mainly focus on the high-emission pathways (SSP5-8.5 for CMIP6 and RCP8.5 for CMIP5), because they can allow us to respond to climate extremes to high-level warming (e.g., 3 °C above pre-industrial). SSP5-8.5 for CMIP6 and RCP8.5 for CMIP5 are high-emission scenarios with the same radiative forcing of 8.5 W/m^2 by 2100. Although SSP5-8.5 shows about 20% higher CO_2 emissions by the end of the century and lower emissions of other greenhouse gases, they are close to each other.

To assess the ability of the models to simulate precipitation, daily precipitation in 1986-2005 from the APHRODITE (Asian Precipitation-Highly Resolved Observational Data Integration Towards Evaluation of Water Resources) dataset is used. APHRODITE, with a spatial resolution of 0.25°× 0.25°, is a high-resolution and long-time (since 1951) land precipitation gridding data covering the entire Asian region. At present, the dataset has been applied to the research on climate change and the

water cycle, and the test of high-resolution model results (Xu et al., 2016; Du et al., 2022; Tan et al., 2021).

The dataset of land use includes four periods 1990, 1995, 2000, and 2005. The Landsat TM/ETM remote sensing images of each period are used as the main data source and generated through manual visual interpretation. DEM data is derived from the Resource Data Cloud Platform (http://www.resdc.cn/). The soil data and Normalized Difference Vegetation Index (NDVI) data are developed by the National Tibetan Plateau Data Center (http://data.tpdc.ac.cn/). Land-Use Harmonization 1 (LUH1) (https://doi.org/10.3334/ORNLDAAC/1248) and Land-Use Harmonization 2 (LUH2) (https://luh.umd.edu/) are used for the CMIP5 and CMIP6 simulations of land use states. In preparation for CMIP5, the LUH1(Chini et al., 2014) project provided harmonized land use data for the years 1500–2100 at 0.5◦ × 0.5◦ resolution. Land use categories of cropland, pasture, primary land, secondary (recovering) land, urban land, and underlying annual land-use transitions are included. Building upon previous work from CMIP5, for which the original LUH1 dataset was used, LUH2 (Hurtt et al., 2020) has updated inputs from the History of the Global Environment database (HYDE) for historical agricultural patterns, a new historical wood harvest reconstruction, new maps, and 20 rates of shifting cultivation, extends the timespan to 850-2100 at 0.25×0.25°, and constrains the forest cover gross transitions using remote sensing observations. In addition, LUH2 includes 12 different land-use types (i.e. forested and non-forested primary and secondary land, cropland of C3 annual, C3 perennial, C4 annual, C4 perennial, and C3 nitrogen-fixing, urban, managed pasture and rangeland) and includes transitions between all combinations of these categories.

2.3 Methodology

The RUSLE was developed in the 1980s by the U.S. Department of Agriculture Agricultural Research Service (USDA-ARS) (Renard et al., 1991) (Renard, 1997). Supported by the geographical information system (GIS) and remote sensing (RS) technologies, the RUSLE model has been extensively used to estimate long-term annual soil erosion under many scenarios (Millward & Mersey, 1999) and at multiple scales (Wang et al., 2021). Studies have confirmed the applicability and reliability of the model in China (Wang et al., 2021). This paper adopted the RUSLE model to estimate the soil erosion in China from 1986-2005 and 2031-2050 (Tang et al., 2015; Xue et al., 2018; Ghosal and Das, 2020), and the model can be expressed as follows:

$$A = R \times LS \times K \times C \times P$$

A is the annual soil erosion ($t \cdot hm^{-2} \cdot a^{-1}$). R is the rainfall erosivity factor ($MJ \cdot mm \cdot hm^{-2} \cdot h^{-1} \cdot a^{-1}$). A universal rainfall erosivity calculation method based on daily rainfall data from 71 representative meteorological stations across China is applied in this study (Zhang et al., 2002). K is the soil erodibility factor ($t \cdot hm^{2} \cdot h \cdot MJ^{-1} \cdot hm^{-2} \cdot mm^{-1}$), which can be calculated using the formula proposed by (Williams, 1990). C is the cover management factor and the C factor in this paper was updated based on the method (Knijff et al., 2000). LS is the average topographical parameter that combines the slope length and steepness (dimensionless) by referring to the method of (Liu et al., 1994). P is the conservation support practice factor.

3 Results

3.1 Historical simulation of soil erosion

Fig.2 shows the spatial distribution of annual mean soil erosion over China derived from observation data, CMIP5, and CMIP6 models for the period from 1986-2005. The figure of observation shows that annual soil erosion is relatively low over Northeast China's black soil region, increasing southeastward and reaching the maximum in the Qinghai-Tibet Plateau region and Northwest China

Loess Plateau region. The study area's average annual total soil erosion for the base period (1986 to 2005) is 55.89 $t \cdot hm^{-2} \cdot a^{-1}$. Compared to observation data, CMIPs simulate the annual soil erosion in a similar spatial pattern, both of which can capture regional and local behaviors of high-intensity soil erosion across China. There is no apparent improvement in CMIP6 models in capturing the spatial pattern and direction of changes in the observation data (Gusain et al., 2020). However, the average soil erosion of 1986-2005 in CMIP5 and CMIP6 are 364.79, 477.97$t \cdot hm^{-2} \cdot a^{-1}$. The simulated soil erosion is higher than the observations over most areas, especially in the Qinghai-Tibet Plateau region. This is mainly because the observation data is obtained by interpolating the measured rainfall data of the rainfall stations, but there are few rainfall stations in the Qinghai-Tibet Plateau which could lead to great uncertainty in the interpolation.

An overestimation of rainfall erosivity (34%-71% higher) and underestimation of the conservation support practice factor (16%-19% lower) for all of China are estimated by CMIPs compared with the observations. Only the spatial patterns of rainfall erosivity in CMIP6 for a few areas are closer to the observations than in CMIP5. The RCM of CMIP5 fails to capture the orographic effects and local change in the landmass that influences the spatial variability and distribution of rainfall (Zhu et al., 2020; Jain et al., 2019; Wang et al., 2022). This will lead to an underestimation of extreme rainfall by the RCM. Latest studies have also shown that an improvement is observed in CMIP6 over CMIP5 in simulating the spatial variability of average mean precipitation over the dry areas and high rainfall receiving areas (Gusain et al., 2020). CMIP6 simulation results pay more attention to the influence of rainfall erosivity on soil erosion, especially the critical soil and water loss caused by heavy rainfall events. For the P factor, the decreased difference from observation is found in arid and semiarid regions of China from CMIP5 to CMIP6. The new version of Land-Use Harmonization 2 is completely updated with new inputs and includes higher spatial resolution, increased detail (12 states vs. 5 and all associated transitions), and added management layers (Hurtt et al., 2020). The newly added management factors for CMIP6 are conducive to better evaluating the P factor.

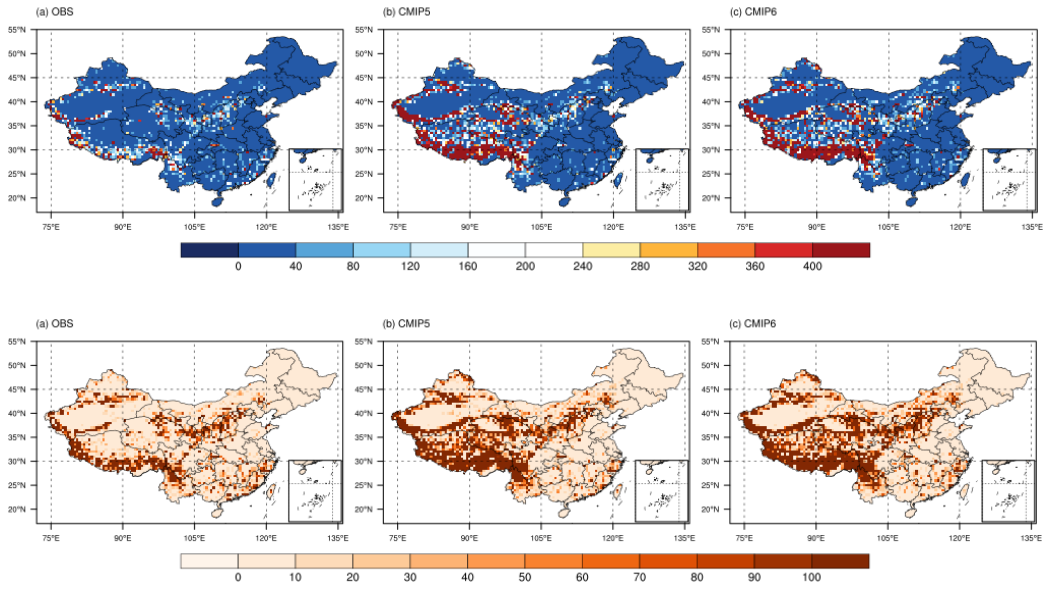

Fig.2 Spatial patterns of soil erosion (unit: $t \cdot km^{-2} \cdot a^{-1}$) from (a) observation, (b) CMIP5 model and(c) CMIP6 model over China for 1986-2005

Tab.1 Factors A, R, and P of each area from (a) observation, (b) CMIP5 model, and (c) CMIP6

model over China for 1986-2005

Area	A ($t \cdot km^{-2} \cdot a^{-1}$)			R ($MJ \cdot mm \cdot hm^{-2} \cdot h^{-1} \cdot a^{-1}$)			P		
	OBS	CMIP5	CMIP6	OBS	CMIP5	CMIP6	OBS	CMIP5	CMIP6
Ⅰ	0.85	2.03	2.21	548.85	1723.70	1663.90	0.79	0.71	0.69
Ⅱ	20.64	33.19	30.12	1226.00	1432.80	2520.70	0.59	0.60	0.33
Ⅲ	71.53	96.75	141.72	416.00	667.76	1251.30	0.76	0.54	0.53
Ⅳ	61.20	380.49	243.83	51.57	236.27	205.27	0.97	0.75	0.84
Ⅴ	30.19	19.13	19.21	4670.40	3330.30	3752.20	0.70	0.69	0.61
Ⅵ	24.97	24.39	66.85	1947.70	1373.90	3294.60	0.73	0.67	0.68
Ⅶ	42.40	62.07	74.79	1930.00	2740.60	2490.60	0.85	0.72	0.77
Ⅷ	148.34	1288.00	2174.50	196.37	1466.80	1780.40	0.98	0.65	0.80
China	55.89	364.79	477.97	1004.30	1347.60	1718.50	0.85	0.69	0.71

This study uses a Taylor diagram (Taylor, 2001) to quantify the pattern similarity between two variables (i.e., soil erosion from observations and CMIPs). The Taylor diagram provides a concise statistic summary of how well the pattern distribution of the two variables matches. The diagram visualizes the degree of correlation (pattern correlation coefficient, PCC), centered root mean square error (RMSE), and the ratio of spatial standard deviation (RSD). In this study, the Taylor diagram was used to visualize and evaluate the soil erosion performance of CMIP5 and CMIP6 over each erosion region. The ability of the two CMIP models to estimate annual soil erosion is presented as Taylor diagrams (Fig.3). 'REF' on the x-axis represents the observation data (observation). As shown in Fig.3, both CMIP5 and CMIP6 offer good performance in reproducing soil erosion in the Northeast China black soil region and the Southwest China karst region. The PCCs between the simulation and observation are greater than 0.90, the centered RMSEs are generally less than 0.25, and the RSDs mainly vary from 1 to 1.25. Results of CMIPs have lower PCCs and higher RMSEs over the North China sandstorm region, Southwest China purple soil region, and Qinghai-Tibet Plateau region compared with the results of the other five regions. Overall, CMIP6 shows slight improvements, compared to CMIP5, in simulating the spatial pattern for soil erosion, especially in the Northeast China black soil region, and Northwest China Loess Plateau region with higher PCCs and lower RSDs. In conclusion, compared with CMIP5, limited improvements in reproducing soil erosion are found in CMIP6. The high-resolution GCM results of CMIP6 are closer to the observed values than the high-resolution RCM results of CORDEX. This suggests that the most recent GCM offered by CMIP6 can enhance local simulation details while better capturing the relationship between large-scale and mesoscale circulation. Therefore, CMIP6's high-resolution GCM can provide more reliable climate system simulation and projection. The horizontal resolution of the model does not change from the RCM of CMIP5 to the GCM of CMIP6. In terms of relative aspects, the better performance of climate models in capturing climate variables and soil erosion characteristics is more likely associated with the representation of physical processes in climate models from CMIP6 (Su et al., 2021).

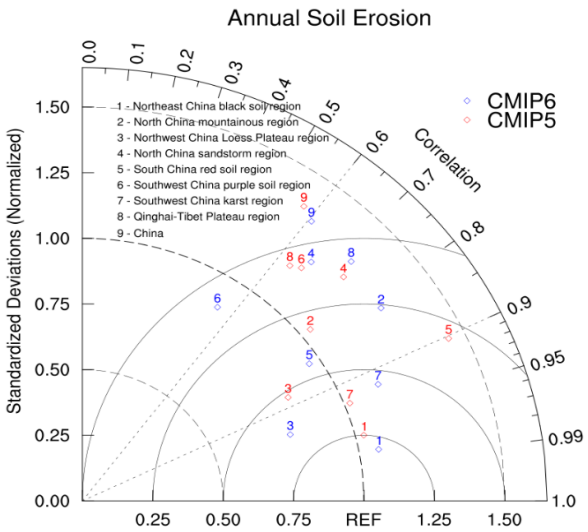

Fig.3 Taylor diagram of the spatial distribution of annual soil erosion for CMIP5 and CMIP6 models

3.2 Future projections of soil erosion

The CMIP5 and CMIP6 outputs of soil erosion were used to estimate the projected percentage of change for the near future (2031-2050) compared to the base period over China (Fig.4). In terms of the spatial distribution of changes, results show that almost all regions expect an increase of soil erosion under the RCP8.5 and SSP5-8.5. They both projected the largest increase in soil erosion over the Qinghai-Tibet Plateau region. But CMIP6 projected a less amount of positive change in soil erosion than projected by CMIP5 models. Relative to 1986-2005, areal-mean soil erosion would increase by approximately 27.85 and 20.03 $t \cdot hm^{-2} \cdot a^{-1}$ over China for RCP8.5 and SSP5-8.5, respectively. Furthermore, the change in soil erosion in a few parts of eastern China is not consistent between the two CMIPs. According to the latest version CMIP6 and the extreme scenario SSP5-8.5, soil erosion over the Northeast China black soil region, Southwest China purple soil region, and Southwest China karst region signalize 4.54%, 2.88%, and 1.62% decrease for 2031-2050 relative to 1986-2005. Contrary to CMIP6, CMIP5 estimates that these areas will increase by 15-21% under the RCP8.5 climate scenario. Under the framework of CMIP6, LUH2 pays more attention to the influence of management factors on land use. The introduction of human disturbance and the slow increase of rainfall erosivity result in the intensified soil erosion simulated by CMIP6 is less than that simulated by CMIP5. CMIP6 model takes more parameters into account, so its simulated soil erosion change needs more attention.

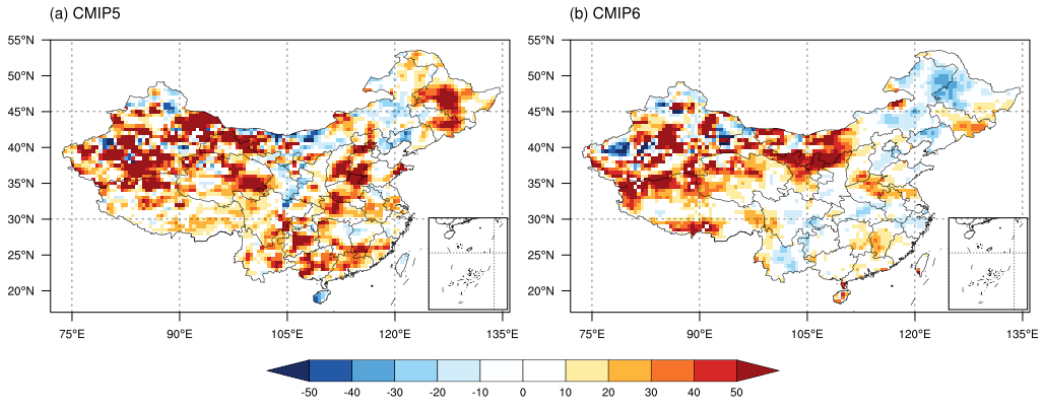

Fig.4 Relative percentage changes for 2031-2050 relative to 1986-2005 in annual soil erosion (unit: $t \cdot km^{-2} \cdot a^{-1}$) projected by CMIP5 and CMIP6 models

3.3 Effects of climate and land use change on soil erosion

In the process of projecting changes in soil erosion in the study area, it is considered that climate warming affects the R and P factors in the RUSLE model mainly by changing rainfall and land use types. Through the control variate method, the contribution rates of rainfall and land use to soil erosion changes can be calculated by exploring one factor while remaining the other unchanged. The results are shown in the following Fig.5. According to the CMIP5 simulation, the contribution rate of rainfall change to the aggravation of soil erosion in the study area is as high as 51.68%, while the contribution rate of land use is only -5.92%. Both climate change and land use change affect soil erosion and its spatial distribution. The impact of climate change is far greater than that of land use change. Compared with CMIP5, CMIP6 amplifies the negative effect of land use, with a contribution rate of -13.77%, while reducing the positive effect of rainfall, with a contribution rate of only 35.74%.

For rainfall erosivity, regions showing obvious differences between CMIP6 and CMIP5 are mainly located in a few areas of the Southwest China karst region, Northwest China Loess Plateau region, and Northeast China black soil region, where the magnitude of the difference is respectively 75.34%, 74.63%, and 63.53%. Among them, it is worth noting that the future response of extreme rainfall to warming in the Northwest China Loess Plateau region by CMIP6 (72.67%) is large than by CMIP5 (-1.96%). CMIP6 and CMIP5 simulated climate changes in these three regions have opposite contributions to soil erosion. This is related to the opposite variation of erosive rainfall simulated by the two models. CMIP6 simulation results show that the erosive rainfall in the Southwest China karst region and Northeast China black soil region during 2031-2050 will decrease compared with the historical period, and in other areas will further increase compared with CMIP5. As the most active factor in the process of soil erosion, changes in precipitation can directly lead to changes in soil erosion, and the change rate of the latter can be several times of the former. A 4% to 18% increase in precipitation can cause a 31% to 167% increase in soil loss (Zhang, 2007). Considering the superiority of CMIP6 compared with CMIP5, it is necessary to timely optimize the soil and water conservation work in each region according to the simulation results of CMIP6.

Land use change can either lead to a further increase in soil erosion (agricultural expansion and deforestation) or a decrease (agricultural abandonment and reforestation) (Eekhout and de Vente, 2022). But if we only discuss the P factor, with the improvement of human awareness of protecting the ecological environment, taking scientific and reasonable soil and water conservation measures will help to achieve the effect of controlling soil and water loss. In near future for all regions except the Qinghai-

Tibet Plateau region, the negative effect of the P factor on soil erosion in SSP5-8.5 are larger than those in RCP8.5. The largest differences are found in Southwest China purple soil region. Under the SSP5-8.5 climate scenario, more land in the region has changed from natural vegetation that has never been affected by human activities to non-forest land that has gradually recovered under human interference. The area of purple soil area is smaller than that of other areas (such as black soil area), so the change proportion of the same volume of land in the whole area will become particularly prominent. Additionally, due to the unique fertile soil conditions of black soil and purple soil, protective agriculture must be actively carried out in the farming area to ensure food security in the future. Currently, the relative share of conservation agriculture of total global cropland is estimated at 12.5%, with a clear increasing trend since the mid-1990s (Kassam et al., 2019). The soil conservation practice scenario shows a potential overall offset of the estimated soil erosion increase of about 64% (Borrelli et al. 2017). Soil conservation measures are often promoted as a solution to adapt to the projected increase of soil erosion under climate change (Amundson et al., 2015), which may include land use change, such as reforestation, and a range of on-site and off-site measures (Xiong et al., 2018). The future projections of soil loss rates could be at least 16% higher if land use changes are ignored. Therefore, it is recommended that projections of soil losses due to water erosion should consider both a wide range of climate change scenarios but also future land use changes.

Tab.2 Contributions of land use and climate changes to soil erosion in each area

Area	Climate change		Land use change	
	CMIP5	CMIP6	CMIP5	CMIP6
Ⅰ	52.98	-10.55	-6.99	-17.34
Ⅱ	41.31	45.85	-16.48	-35.17
Ⅲ	-1.96	72.67	22.61	-15.06
Ⅳ	48.38	41.38	-0.46	-6.15
Ⅴ	61.86	45.90	-20.40	-33.18
Ⅵ	52.56	20.67	-11.19	-51.03
Ⅶ	72.16	-3.19	-9.17	-12.21
Ⅷ	72.68	52.36	0.70	7.72
China	51.68	35.74	-5.92	-13.77

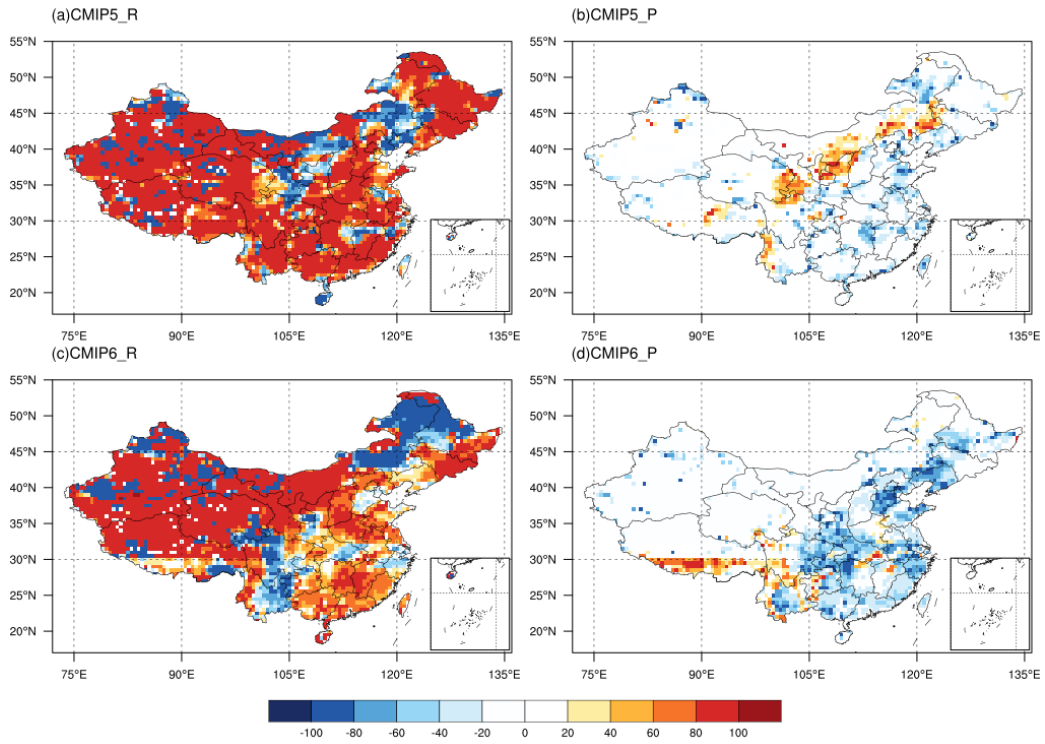

Fig.5 The contribution of climate change and land use change to soil erosion under RCP8.5 and SSP5-8.5

4 Conclusion

This study compares a 50km global climate model from CMIP6 and a 50km regional climate model from CMIP5 in terms of simulating and projecting soil erosion response to climate and land-use changes. Special attention is paid to the differences in the effects of land use change and precipitation change on soil erosion under different emission scenarios. The main findings are summarized as follows:

(1) Our diagnostics from both CMIP5 and CMIP6 show that there are increases in soil erosion over China for a future warmer world. We find that both CMIP5 and CMIP6 models capture the observed soil erosion patterns. But the PCC of CMIP6 is slightly larger than that of CMIP5, and the RSD is smaller. The validation results of the high-resolution GCM of CMIP6 are superior to the RCM of CMIP5 with the same resolution because the CMIP6 model not only depicts the finer regional details of processes but also reproduces their interaction with large mesoscale circulation.

(2) Both models project increased soil erosion in China for 2031-2050 relative to 1986-2005, but the value projected under SSP5-8.5 is less than that under RCP8.5. The average projected increases in soil erosion are 27.85 derived from CMIP5 and 20.03 t·hm-2·a-1 derived from CMIP6 models with remarkable geographical heterogeneity. We assess that the CMIP6 projections provide a less severe soil erosion situation with better performance in reproducing observational patterns. It is recommended to the decision-makers to update impact studies for water and soil conservation performed using CMIP5 with the CMIP6 high-resolution model.

(3) The contribution rates of land use change and climate change to soil erosion projected by CMIP models are quantified. Land use and climatic changes contributed 51.68% and -5.92% respectively from CMIP5 simulations while 35.74% and -13.77% from CMIP6 to the increased soil

371 erosion rate. The negative contribution of land use change is gradually intensified with CMIP6 models
372 representing finer-scale processes of converting land-use type into cropland, pasture, and urban land.
373 Therefore, impact studies for soil erosion based on the CMIP5 projections would benefit from updating
374 to the CMIP6 high-resolution model to get more confidence in estimating future climate and land-use
375 conditions. This has important implications for policymakers and stakeholders who will have to weigh
376 the uncertainty of climate and land-use change in their decisions.
377

378 ## Acknowledgments

379 This study was supported by the Guangzhou Basic and Applied Basic Research Foundation
380 (Grant No. 202201011403), the Fundamental Research Funds for the Central Universities-Sun Yat-Sen
381 University (Grant No. 22qntd2001), and the Hong Kong Research Grants Council Early Career Scheme
382 (Grant No. PP5Z). Data used in this paper is freely available at Mendeley Data
383 (DOI:10.17632/w948kfrsv6.1). We acknowledge and thank the climate modeling groups in the
384 Coordinated Regional Climate Downscaling Experiment and Coupled Model Intercomparison Project
385 for generating their model outputs and making them available. All authors declare no competing
386 financial interests.
387

388 **References**

389 Amundson, R., Berhe, A., Hopmans, J., Olson, C., Sztein, A., Sparks, D. (2015). Soil science. Soil and
390 human security in the 21st century. Science, 348 http://doi.org/10.1126/science.1261071
391 Bai, Z. G., Dent, D. L., Olsson, L. E., Schaepman, M. E. (2008). Global assessment of land degradation
392 and improvement: 1. Identification by remote sensing. Blumea
393 Borrelli, P., Robinson, D. A., Fleischer, L. R., Lugato, E., Ballabio, C., Alewell, C., Meusburger, K.,
394 Modugno, S., Schütt, B., Ferro, V., Bagarello, V., Oost, K. V., Montanarella, L., Panagos, P. (2017).
395 An assessment of the global impact of 21st century land use change on soil erosion. Nature
396 Communications, 8(1), 2013. http://doi.org/10.1038/s41467-017-02142-7
397 Borrelli, P., Robinson, D. A., Panagos, P., Lugato, E., Yang, J. E., Alewell, C., Wuepper, D.,
398 Montanarella, L., Ballabio, C. (2020). Land use and climate change impacts on global soil erosion by
399 water (2015-2070). Proceedings of the National Academy of Sciences of the United States of America,
400 117(36), 21994-22001. http://doi.org/10.1073/pnas.2001403117
401 Boyle, J., Klein, S. A. (2010). Impact of horizontal resolution on climate model forecasts of tropical
402 precipitation and diabatic heating for the TWP-ICE period. Journal of Geophysical Research:
403 Atmospheres, 115(D23) http://doi.org/https://doi.org/10.1029/2010JD014262
404 Chini, L. P., Hurtt, G. C., Frolking, S. (2014). LUH1: Harmonized Global Land Use for Years 1500-
405 2100, V1: ORNL Distributed Active Archive Center.
406 Crosson, P. R. (1995). Soil erosion estimates and costs. Science, 269 5223, 461-464.
407 Dong, T., Dong, W. (2021). Evaluation of extreme precipitation over Asia in CMIP6 models. Climate
408 Dynamics, 57(7), 1751-1769. http://doi.org/10.1007/s00382-021-05773-1
409 Du, Y., Wang, D., Zhu, J., Lin, Z., Zhong, Y. (2022). Intercomparison of multiple high-resolution
410 precipitation products over China: Climatology and extremes. Atmospheric Research, 278, 106342.
411 http://doi.org/https://doi.org/10.1016/j.atmosres.2022.106342
412 Eekhout, J. P. C., de Vente, J. (2022). Global impact of climate change on soil erosion and potential for
413 adaptation through soil conservation. Earth-Science Reviews, 226, 103921.
414 http://doi.org/https://doi.org/10.1016/j.earscirev.2022.103921
415 Ghosal, K., Das Bhattacharya, S. (2020). A Review of RUSLE Model. Journal of the Indian Society of
416 Remote Sensing, 48(4), 689-707. http://doi.org/10.1007/s12524-019-01097-0
417 Gusain, A., Ghosh, S., Karmakar, S. (2020). Added value of CMIP6 over CMIP5 models in simulating
418 Indian summer monsoon rainfall. Atmospheric Research, 232, 104680.
419 http://doi.org/https://doi.org/10.1016/j.atmosres.2019.104680
420 Haarsma, R. J., Roberts, M. J., Vidale, P. L., Senior, C. A., Bellucci, A., Bao, Q., Chang, P., Corti, S.,
421 Fučkar, N. S., Guemas, V., von Hardenberg, J., Hazeleger, W., Kodama, C., Koenigk, T., Leung, L. R.,
422 Lu, J., Luo, J. J., Mao, J., Mizielinski, M. S., Mizuta, R., Nobre, P., Satoh, M., Scoccimarro, E.,
423 Semmler, T., Small, J., von Storch, J. S. (2016). High Resolution Model Intercomparison Project
424 (HighResMIP v1.0) for CMIP6. Geoscientific Model Development, 9(11), 4185-4208.
425 http://doi.org/10.5194/gmd-9-4185-2016
426 Haarsma, R., Roberts, M., Vidale, P. L., Senior, C., Bellucci, A., Bao, Q., Chang, P. P., Corti, S.,
427 Fuckar, N., Guemas, V., Hardenberg, J., Hazeleger, W., Kodama, C., Koenigk, T., Leung, L., Lu, J.,
428 Luo, J., Mao, J., Mizielinski, M., Storch, J. (2016). High Resolution Model Intercomparison Project
429 (HighResMIP v1.0) for CMIP6. Geoscientific Model Development, 9, 4185-4208.
430 http://doi.org/10.5194/gmd-9-4185-2016
431 Hartmann, D. L. (2016). Chapter 11 - Global Climate Models. In D. L. Hartmann (Ed.), Global

Physical Climatology (Second Edition) (325-360). Elsevier.
http://doi.org/https://doi.org/10.1016/B978-0-12-328531-7.00011-6.
Hurtt, G. C., Chini, L., Sahajpal, R., Frolking, S., Bodirsky, B. L., Calvin, K., Doelman, J. C., Fisk, J., Fujimori, S., Klein Goldewijk, K., Hasegawa, T., Havlik, P., Heinimann, A., Humpenöder, F., Jungclaus, J., Kaplan, J. O., Kennedy, J., Krisztin, T., Lawrence, D., Lawrence, P., Ma, L., Mertz, O., Pongratz, J., Popp, A., Poulter, B., Riahi, K., Shevliakova, E., Stehfest, E., Thornton, P., Tubiello, F. N., van Vuuren, D. P., Zhang, X. (2020). Harmonization of global land use change and management for the period 850 – 2100 (LUH2) for CMIP6. Geoscientific Model Development, 13(11), 5425-5464. http://doi.org/10.5194/gmd-13-5425-2020
Hurtt, G., Chini, L., Sahajpal, R., Frolking, S., Bodirsky, B., Calvin, K., Doelman, J., Fisk, J., Fujimori, S., Klein Goldewijk, K., Hasegawa, T., Havlik, P., Heinimann, A., Humpenöder, F., Jungclaus, J., Kaplan, J., Kennedy, J., Krisztin, T., Lawrence, D., Tubiello, F. (2020). Harmonization of global land use change and management for the period 850-2100 (LUH2) for CMIP6. Geoscientific Model Development, 5425-5464. http://doi.org/10.5194/gmd-13-5425-2020
Jain, S., Salunke, P., Mishra, S. K., Sahany, S., Choudhary, N. (2019). Advantage of NEX-GDDP over CMIP5 and CORDEX Data: Indian Summer Monsoon. atmospheric research, 228, 152-160. http://doi.org/https://doi.org/10.1016/j.atmosres.2019.05.026
Kassam, A., Friedrich, T., Derpsch, R. (2019). Global spread of Conservation Agriculture. International Journal of Environmental Studies, 76(1), 29-51. http://doi.org/10.1080/00207233.2018.1494927
Knijff, J., Jones, R., Montanarella, L. (2000). Soil Erosion Risk Assessment in Europe. Soil Erosion Risk Assessment in Europe
Liu, B., Nearing, M., Risse, M. (1994). Slope Gradient Effects on Soil Loss for Steep Slopes. Transactions of the ASAE, 37, 1835-1840. http://doi.org/10.13031/2013.28273
Luetzenburg, G., Bittner, M. J., Calsamiglia, A., Renschler, C. S., Estrany, J., Poeppl, R. (2020). Climate and land use change effects on soil erosion in two small agricultural catchment systems Fugnitz – Austria, Can Revull – Spain. Science of the Total Environment, 704, 135389. http://doi.org/https://doi.org/10.1016/j.scitotenv.2019.135389
Maeda, E. E., Pellikka, P. K. E., Siljander, M., Clark, B. J. F. (2010a). Potential impacts of agricultural expansion and climate change on soil erosion in the Eastern Arc Mountains of Kenya. Geomorphology, 123(3), 279-289. http://doi.org/https://doi.org/10.1016/j.geomorph.2010.07.019
Maeda, E. E., Pellikka, P. K. E., Siljander, M., Clark, B. J. F. (2010b). Potential impacts of agricultural expansion and climate change on soil erosion in the Eastern Arc Mountains of Kenya. Geomorphology, 123(3), 279-289. http://doi.org/https://doi.org/10.1016/j.geomorph.2010.07.019
Millward, A. A., Mersey, J. E. (1999). Adapting the RUSLE to model soil erosion potential in a mountainous tropical watershed. Catena, 38(2), 109-129. http://doi.org/https://doi.org/10.1016/S0341-8162(99)00067-3
Moss, R. H., Edmonds, J. A., Hibbard, K. A., Manning, M. R., Rose, S. K., van Vuuren, D. P., Carter, T. R., Emori, S., Kainuma, M., Kram, T., Meehl, G. A., Mitchell, J. F. B., Nakicenovic, N., Riahi, K., Smith, S. J., Stouffer, R. J., Thomson, A. M., Weyant, J. P., Wilbanks, T. J. (2010). The next generation of scenarios for climate change research and assessment. Nature, 463(7282), 747-756. http://doi.org/10.1038/nature08823
Naipal, V., Ciais, P., Wang, Y., Lauerwald, R., Guenet, B., Van Oost, K. (2018). Global soil organic carbon removal by water erosion under climate change and land use change during AD 1850 –

2005. Biogeosciences, 15(14), 4459-4480. http://doi.org/10.5194/bg-15-4459-2018
Nikiema, P. M., Sylla, M. B., Ogunjobi, K., Kebe, I., Gibba, P., Giorgi, F. (2017). Multi-model CMIP5 and CORDEX simulations of historical summer temperature and precipitation variabilities over West Africa. International Journal of Climatology, 37(5), 2438-2450. http://doi.org/https://doi.org/10.1002/joc.4856
Oldeman, L. R., Hakkeling, R. T. A., Sombroek, W. G. (1990), World map of the status of human-induced soil degradation: an explanatory note.
O'Neill, B. C., Tebaldi, C., van Vuuren, D. P., Eyring, V., Friedlingstein, P., Hurtt, G., Knutti, R., Kriegler, E., Lamarque, J. F., Lowe, J., Meehl, G. A., Moss, R., Riahi, K., Sanderson, B. M. (2016). The Scenario Model Intercomparison Project (ScenarioMIP) for CMIP6. Geoscientific Model Development, 9(9), 3461-3482. http://doi.org/10.5194/gmd-9-3461-2016
Pal, S. C., Chakrabortty, R., Roy, P., Chowdhuri, I., Das, B., Saha, A., Shit, M. (2021). Changing climate and land use of 21st century influences soil erosion in India. Gondwana Research, 94, 164-185. http://doi.org/https://doi.org/10.1016/j.gr.2021.02.021
Renard, K. G. (1997). Predicting soil erosion by water: A guide to conservation planning with the Revised Universal Soil Loss equation (RUSLE). Predicting soil erosion by water: A guide to conservation planning with the Revised Universal Soil Loss equation (RUSLE).
Renard, K. G., Foster, G. R., Weesies, G. A., Porter, J. P. (1991). RUSLE: Revised universal soil loss equation. Journal of Soil and Water Conservation, 46(1), 30.
Rivington, M., Miller, D., Matthews, K. B., Russell, G., Bellocchi, G., Buchan, K. (2008). Evaluating regional climate model estimates against site-specific observed data in the UK. climatic change, 88(2), 157-185.
Schlund, M., Lauer, A., Gentine, P., Sherwood, S. C., Eyring, V. (2020). Emergent constraints on equilibrium climate sensitivity in CMIP5: do they hold for CMIP6? Earth System Dynamics, 11(4), 1233-1258. http://doi.org/10.5194/esd-11-1233-2020
Su, B., Huang, J., Mondal, S. K., Zhai, J., Wang, Y., Wen, S., Gao, M., Lv, Y., Jiang, S., Jiang, T., Li, A. (2021). Insight from CMIP6 SSP-RCP scenarios for future drought characteristics in China. Atmospheric Research, 250, 105375. http://doi.org/https://doi.org/10.1016/j.atmosres.2020.105375
Tan, M. L., Gassman, P. W., Liang, J., Haywood, J. M. (2021). A review of alternative climate products for SWAT modelling: Sources, assessment and future directions. Science of the Total Environment, 795, 148915. http://doi.org/https://doi.org/10.1016/j.scitotenv.2021.148915
Tang, Q., Xu, Y., Bennett, S. J., Li, Y. (2015). Assessment of soil erosion using RUSLE and GIS: a case study of the Yangou watershed in the Loess Plateau, China. Environmental Earth Sciences, 73(4), 1715-1724. http://doi.org/10.1007/s12665-014-3523-z
Taylor, K. E. (2001). Summarizing multiple aspects of model performance in a single diagram. Journal of Geophysical Research: Atmospheres, 106(D7), 7183-7192. http://doi.org/https://doi.org/10.1029/2000JD900719
Vizy, E. K., Cook, K. H., Crétat, J., Neupane, N. (2013). Projections of a Wetter Sahel in the Twenty-First Century from Global and Regional Models. Journal of Climate, 26(13), 4664-4687. http://doi.org/10.1175/JCLI-D-12-00533.1
Wang, L., Li, Y., Li, M., Li, L., Liu, F., Liu, D. L., Pulatov, B. (2022). Projection of precipitation extremes in China's mainland based on the statistical downscaled data from 27 GCMs in CMIP6. Atmospheric Research, 280, 106462. http://doi.org/https://doi.org/10.1016/j.atmosres.2022.106462
Wang, Z., Zeng, Y., Li, C., Yan, H., Yu, S., Wang, L., Shi, Z. (2021). Telecoupling cropland soil

erosion with distant drivers within China. Journal of Environmental Management, 288, 112395. http://doi.org/https://doi.org/10.1016/j.jenvman.2021.112395

Williams, J. R. (1990). EPIC-erosion/productivity impact calculator: 1. Model documentation. Technical Bulletin - United States Department of Agriculture, 4(4), 206-207.

Xin, X., Wu, T., Jie, W., Zhang, J. (2021). Impact of Higher Resolution on Precipitation over China in CMIP6 HighResMIP Models. Atmosphere, 12(6), 762.

Xiong, M., Sun, R., Chen, L. (2018). Effects of soil conservation techniques on water erosion control: A global analysis. Science of the Total Environment, 645, 753-760. http://doi.org/https://doi.org/10.1016/j.scitotenv.2018.07.124

Xu, H., Xu, C., Chen, S., Chen, H. (2016). Similarity and difference of global reanalysis datasets (WFD and APHRODITE) in driving lumped and distributed hydrological models in a humid region of China. Journal of Hydrology, 542, 343-356. http://doi.org/https://doi.org/10.1016/j.jhydrol.2016.09.011

Xue, J., Lyu, D., Wang, D., Wang, Y., Yin, D., Zhao, Z., Mu, Z. (2018). Assessment of Soil Erosion Dynamics Using the GIS-Based RUSLE Model: A Case Study of Wangjiagou Watershed from the Three Gorges Reservoir Region, Southwestern China Water (10, pp.).

Zhi, Li, Wen-Zhao, Liu, Xun-Chang, ZhangFen-Li, Zheng. (2011). Assessing the site-specific impacts of climate change on hydrology, soil erosion and crop yields in the Loess Plateau of China. Climatic Change

Zhu, H., Jiang, Z., Li, J., Li, W., Sun, C., Li, L. (2020). Does CMIP6 Inspire More Confidence in Simulating Climate Extremes over China? Advances in Atmospheric Sciences, 37(10), 1119-1132. http://doi.org/10.1007/s00376-020-9289-1